MODELING AND SIMULATION OF RAILWAY BOGIE STRUCTURAL VIBRATIONS

H. CLAUS and W. SCHIEHLEN*

SUMMARY

The method of multibody systems including flexible bodies is applied to a railway bogie of the German high-speed train ICE. The flexible elements like the bogie frame are characterized by shape integrals which are evaluated prior to time integration to improve computational efficiency. The eigenbehavior of the railway bogie with a flexible bogie frame, rigid wheelsets and a rigid car body is analyzed in detail. An overview is given how the equations describing the bogie dynamics are derived. The representation of track irregularities by power spectral density functions is discussed and compared with measurement data. The structural vibrations of the railway bogie are primarily excited by the tracks. These forced vibrations resulting in stress and fatigue of the bogie frame are investigated by simulations.

1 INTRODUCTION

Investigation of system dynamics and their long time effects on bogies, tracks and foundations is an important topic in railway engineering using modeling and simulation techniques. The method of multibody system dynamics is well suited to model railway vehicles in the low frequency range. The resulting equations of motion may be analyzed by different methods. A popular approach is time integration, see e.g. Popp, Schiehlen [11], allowing nonlinear models and any kind of excitation. This method was e.g. applied by Luo, Babbitas, Brickle [9] to analyze a metro railway vehicle bogie. Other approaches for stochastic excitation are e.g. the direct covariance method (time domain) or the power spectral density method (frequency domain) respectively, see e.g. Diepen [4] and Stichel [14]. The application of these methods is limited to linear models and stationary stochastic excitations.

*Institute B of Mechanics, University of Stuttgart, Germany

Traveling at higher speeds leads to forced vibrations in a wide frequency range requiring an analysis of the middle and high frequency vibrations and the corresponding noise, too. The brumming noise which may affect passengers in the coach is found to be due to noncircular wheels, see Zacher [17]. Such a noise indicates that the bogie frame is also subject to middle frequency excitations. In this paper the ICE bogie MD 530 is modeled and simulated to learn more about its general behavior in the range of middle frequencies. For these investigations the method of the flexible multibody systems has to be applied which consider the elastic properties of the bogie additionally to the rigid body dynamics.

The frame of the bogie MD 530 is a welded steel box with a complex geometry. Thus, the finite element method is well suited to describe its structural properties, see Ehrmann [5]. In addition, the multibody system approach allows to model large motions and nonlinear interactions between the bogie components. With a railway bogie the wheelsets are subject to large rotation and the suspensions are nonlinear. Therefore, a hybrid modeling should be used which combines the features of a finite element system (FES) and a rigid multibody system (MBS). The method of flexible multibody systems considers complex geometries as well as large motions, see e.g. Shabana [12], and is applied here to a railway bogie. The excitation is implemented as random irregularity of the track geometry based on power spectral density functions published by ARGER/F [1].

2 BOGIE MODELING

The bogie considered consists of an elastic frame, two rigid wheelsets and of the half car body which is modeled as rigid body, too. Figure 1 illustrates three parts of the bogie. The springs and dampers connecting the rigid bodies and the frame are considered as linear. Therefore, for example, the friction damping in the secondary suspension is replaced by linear dampers and the nonlinearity of the springs is neglected.

A floating reference frame is introduced to represent the elastic body within the multibody system. This frame describes the large translational and rotational motions which are nonlinear in general. The elastic deformations are defined relative to this frame. The vector $\boldsymbol{d}$ from the reference frame to a material point is given by

$$\boldsymbol{d}(\boldsymbol{c},t) = \boldsymbol{c} + \boldsymbol{u}(\boldsymbol{c},t) \tag{1}$$

where $\boldsymbol{c}$ indicates the position of the point in the undeformed state and $\boldsymbol{u}$ the displacement vector depending on the reference position $\boldsymbol{c}$ and the time t.

The vector $\boldsymbol{u}$ can be expressed as

$$\boldsymbol{u}(\boldsymbol{c},t) = \boldsymbol{\Phi}(\boldsymbol{c})\boldsymbol{y}_e(t) \tag{2}$$

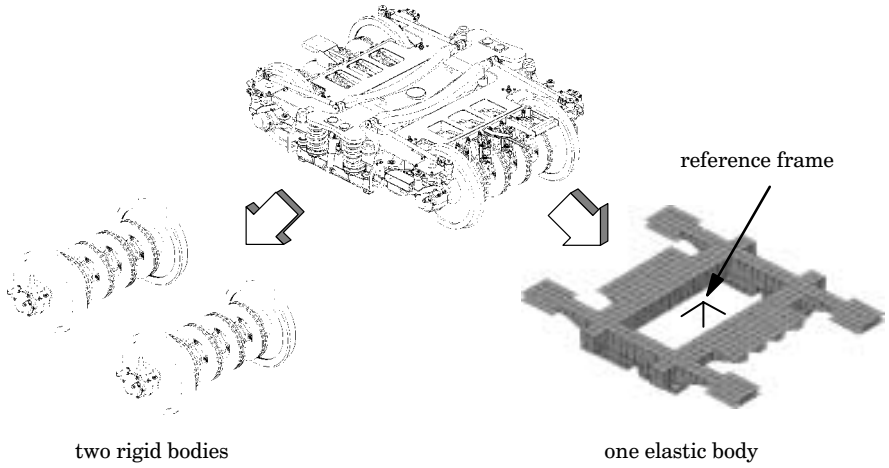

Figure 1: Modeling of the bogie

with the time-invariant shape matrix $\boldsymbol{\Phi}$ and the vector $\boldsymbol{y}_e$ of generalized coordinates of the elastic deformation. The shape matrix $\boldsymbol{\Phi}$ can be obtained through a finite element discretization. Assuming small deformations the relative rotation of a frame rigidly attached to the material point on the elastic body is similarly described as

$$\boldsymbol{A}(\boldsymbol{c},t) = \boldsymbol{I} + \tilde{\boldsymbol{\theta}}(\boldsymbol{c},t) \tag{3}$$

where $\boldsymbol{I}$ denotes the 3×3 idendity matrix and $\tilde{\boldsymbol{\theta}}$ is a skew-symmetric matrix due to the elastic rotational deformations. It is composed by the vector of small rotations $\boldsymbol{\theta} = [\theta_1\, \theta_2\, \theta_3]^T$. This rotation vector can also be expressed by a time invariant shape matrix $\boldsymbol{\Psi}$ and the vector $\boldsymbol{y}_e$ of generalized elastic coordinates as

$$\boldsymbol{\theta}(\boldsymbol{c},t) = \boldsymbol{\Psi}(\boldsymbol{c})\boldsymbol{y}_e(t)\ . \tag{4}$$

The absolute position and orientation of the frame which is attached to a material point of the flexible bogie is given by the vector $\boldsymbol{r}$ and the matrix $\boldsymbol{S}$ as

$$\boldsymbol{r}(\boldsymbol{c},t) = \boldsymbol{r}_1(t) + \boldsymbol{d}(\boldsymbol{c},t) \text{ and} \tag{5}$$

$$\boldsymbol{S}(\boldsymbol{c},t) = \boldsymbol{S}_1(t)\boldsymbol{A}(\boldsymbol{c},t)\ . \tag{6}$$

The vector $\boldsymbol{r}_1$ defines the origin of the floating frame and the matrix $\boldsymbol{S}_1$ the orientation of this frame relative to the inertial frame. The acceleration of the elastic body is derived using the relative kinematics. Considering the rigid and elastic bodies and applying D'Alembert's principle the equations of motion of the system can be written as

$$\boldsymbol{M}(\boldsymbol{y})\ddot{\boldsymbol{y}}(t) + \boldsymbol{k}_c(\boldsymbol{y},\dot{\boldsymbol{y}}) + \boldsymbol{k}_i(\boldsymbol{y}) = \boldsymbol{q}(\boldsymbol{y},\dot{\boldsymbol{y}},t) \tag{7}$$

where the mass matrix $\boldsymbol{M}$, the vector of generalized Coriolis forces $\boldsymbol{k}_c$, the vector of elastic stiffness forces $\boldsymbol{k}_i$ and the vector of other generalized applied forces $\boldsymbol{q}$ are used. The generalized coordinates of the system are assembled in the vector $\boldsymbol{y}$ which comprises the rigid and elastic body coordinates. To obtain the mass matrix various volume integrals of terms including the shape functions and depending on the elastic coordinates have to be computed. Since small deformations are assumed these volume integrals can be expanded into a Taylor series of the elastic coordinates up to first order. The coefficient matrices of the Taylor series, the so-called shape integrals, are calculated by numerical integration. Since the shape integrals do not depend on time, they are computed prior to time integration by pre-processing. A detailed description of the approach can be found in Melzer [10]. The simulation of the system can be carried out using standard time integration techniques.

In this paper the finite element program ANSYS [3] is used to discretize the bogie frame with shell, volume, and beam elements, see Figure 2. The com-

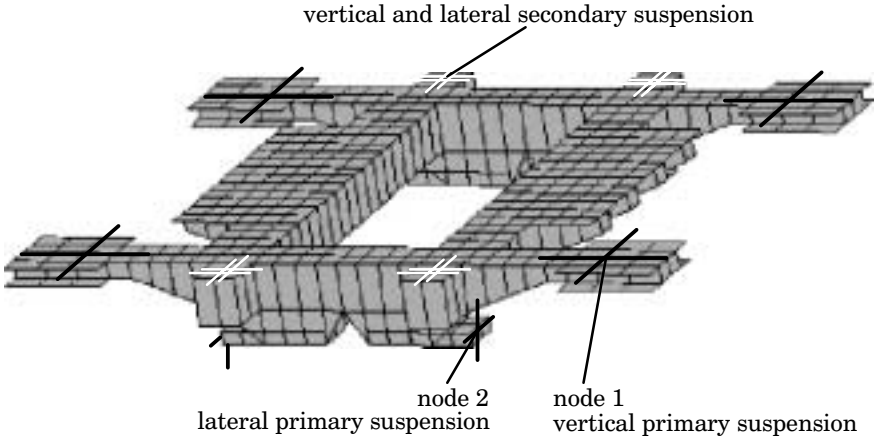

Figure 2: Finite element model of the bogie frame

plex design of the bogie frame is represented by a finite element model with 992 nodes and 1044 elements. Additional heavy parts like the magnetic breaks are modeled separately as beam elements. For the calculation of eigenmodes the total number of degrees of freedom has been adjusted to the so-called master degrees of freedom selected by the program ANSYS applying the Guyan reduction, see Guyan [6]. In addition, nodes where the external forces are applied are chosen, see Figure. In this paper the eigenmodes of the elastic bogie frame are computed considering 1000 master degrees of freedom.

For the analysis of the vehicle system the number of eigenmodes is further reduced by modal condensation to five vertical and five lateral eigenmodes shown in Figure 3. The modal condensation is carried out by the program

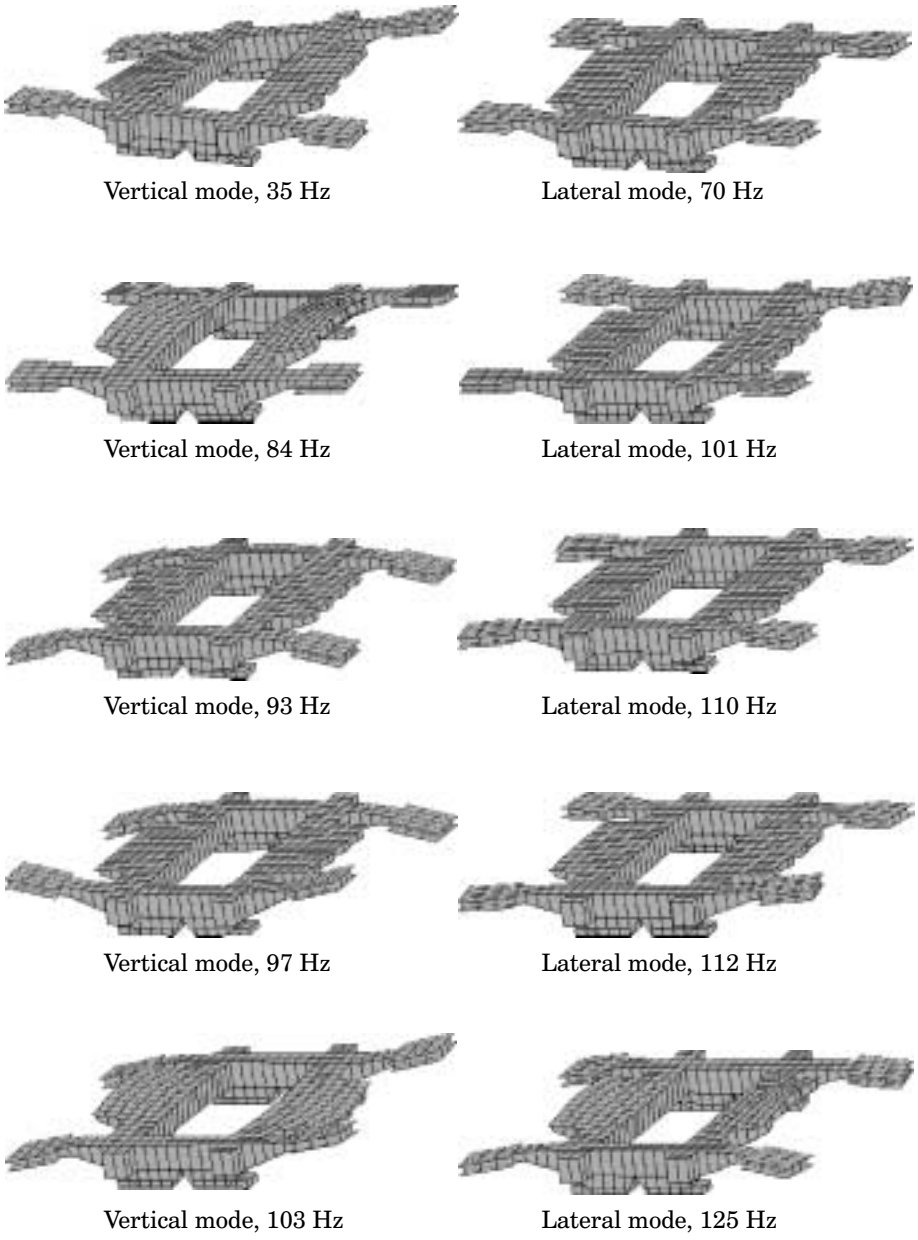

Figure 3: Vertical and lateral eigenmodes of the elastic bogie frame

FEMBS [16] which generates the mode shape matrices and describes them in a standard data format (SID), see Wallrapp [15]. The equations of motion of the flexible multibody system were set up with the symbolical multibody program NEWEUL [8] which includes the mode shape matrices in the SID-format.

Assuming small deformations from the reference position the lateral and horizontal dynamics are decoupled. Therefore, two submodels were set up, one for investigation of the vertical and the other for investigation of the lateral dynamics. In each submodel only the corresponding eigenmodes were applied.

3 EXCITATION BY GEOMETRICAL TRACK IRREGULARITIES

High frequency vibrations of the bogie are excited by irregularities of the track. Numerous measurements have shown that these irregularities represent a stationary stochastic process and they may be described by spectral power density functions. The lateral and vertical profiles of the right and left rail (y_r, z_r, y_l, z_l) result in the track characteristics

$$\zeta_A(x) = (y_r + y_l)/2 \ , \tag{8}$$

$$\zeta_V(x) = (z_r + z_l)/2 \ \text{ and} \tag{9}$$

$$\zeta_C(x) = z_r - z_l \tag{10}$$

where ζ_A means the lateral alignment, ζ_V the vertical profile and ζ_C the cross-level as a function of the longitudinal coordinate x, see also Popp and Schiehlen [11].

The independent excitation profiles can be understood as stochastic Gaussian ergodic processes. Each of the above mentioned ergodic processes $\zeta = \zeta(x)$, $0 \leq x \leq \infty$ are characterized by the mean value

$$\overline{\zeta} = \lim_{L\to\infty} \frac{1}{L} \int_0^L \zeta(x) dx \tag{11}$$

and the correlation function

$$R_\zeta(\xi) = \lim_{L\to\infty} \frac{1}{L} \int_0^L \zeta(x)\zeta(x-\xi) dx \tag{12}$$

which includes for $\xi = 0$ the mean square value

$$\overline{\zeta^2} = \lim_{L\to\infty} \frac{1}{L} \int_0^L \zeta^2(x) dx \ . \tag{13}$$

The Fourier transformation of the correlation function results in the power spectral density S which will be defined as

$$S(\Omega) = \int_{-\infty}^{\infty} R_\xi(\xi) e^{-j\Omega\xi} d\xi \tag{14}$$

where Ω is the distance frequency and, therefore, the coordinate in the frequency domain. Then, the mean square value $\overline{\zeta^2}$ may also be obtained from the spectral density S as

$$\overline{\zeta^2} = \frac{1}{2\pi} \int_{-\infty}^{\infty} S(\Omega) d\Omega \quad . \tag{15}$$

Sometimes the power spectral density is written as

$$\Phi(\Omega) = 2S(\Omega) \tag{16}$$

where the so-called *one-sided* spectral density Φ is defined in the range $\Omega \geq 0$ only. Therefore, the mean square value may be obtained by

$$\overline{\zeta^2} = \frac{1}{2\pi} \int_{0}^{\infty} \Phi(\Omega) d\Omega \quad . \tag{17}$$

Various measurements of track irregularities show that the power spectral densities can be standardized. In ARGER/F [1] analytical power spectral densities are published as *one-sided* density functions,

$$\Phi_{V,A}(\Omega) = A \frac{\Omega_c^2}{(\Omega_r^2 + \Omega^2)(\Omega_c^2 + \Omega^2)} \quad , \tag{18}$$

$$\Phi_C(\Omega) = \frac{A}{l^2} \frac{\Omega_c^2 \Omega^2}{(\Omega_r^2 + \Omega^2)(\Omega_c^2 + \Omega^2)(\Omega_s^2 + \Omega^2)} \tag{19}$$

where $\Phi_{V,A}$ stands for the vertical profile density Φ_V or the lateral alignment density Φ_A respectively. The power spectral density of the cross-level Φ_C is given by equation (19). The length l is half of the reference distance between the rails. The values of the constant factors Ω_c, Ω_r, Ω_s and l are

$$\Omega_c = 0.8246\,\text{rad/m} \quad , \tag{20}$$

$$\Omega_r = 0.0206\,\text{rad/m} \quad , \tag{21}$$

$$\Omega_s = 0.4380\,\text{rad/m} \quad \text{and} \tag{22}$$

$$l = 0.75\,\text{m} \quad . \tag{23}$$

The scalar factor A of the track irregularities is given in ARGER/F [1] as

$$A_{low} = 0.59233 * 10^{-6}\,\text{rad m} \quad \text{and} \tag{24}$$

$$A_{high} = 1.58610 * 10^{-6}\,\text{rad m} \tag{25}$$

where A_{low} stands for a low and A_{high} for a high level of track irregularities. In this paper the factor A is chosen to

$$A = 0.7930 * 10^{-6} \,\mathrm{rad\,m} \tag{26}$$

which is the half of the high level A_{high}. Figure 4 shows some power spectral densities of the measured irregularity profiles and the analytical ones. It has

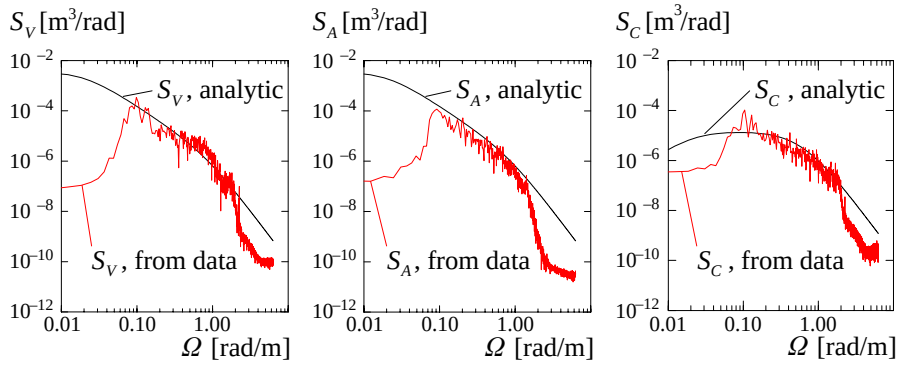

Figure 4: Power spectral densities

to be noted that the measured data represent the track irregularities only for wave lengths between 0.8 m and 84 m. The limitation is due to the measurement equipment and, therefore, valid measured track irregularities are restricted to $0.07\,\mathrm{rad/m} \leq \Omega \leq 2.1\,\mathrm{rad/m}$, see Figure 4. The measurements were made available by the German Railways, Deutsche Bahn AG.

Comparisons of measured data with the analytical power spectral density show good agreement in the valid range of wave length or distance frequencies, respectively. The mentioned distance frequency range corresponds to a frequency range between 0.8 Hz and 23 Hz at a vehicle speed of 250 km/h. The middle frequency dynamics require excitation frequencies up to 150 Hz. For this purpose the analytical spectral densities are used.

Sample functions of stochastic excitation profiles may be generated by the spectral representation method, see e.g. Shinozuka and Deodatis [13]. A modification of this method resulting in a higher computational efficiency is described in Hu and Schiehlen [7]. Applying this modification the sample function can be written as

$$\zeta(x) = \sqrt{2} \sum_{n=0}^{N-1} A_n \cos(\Omega_n x + \varphi_n) \tag{27}$$

considering the spectral density of N discrete frequencies Ω_n. The independent random phase angles $\varphi_n (n = 0, 1, \ldots, N-1)$ are uniformly distributed in the

range $[0, 2\pi]$. The frequencies are set to

$$\Omega_n := n\Delta\Omega = n\frac{\Omega_u}{N} \quad \text{for} \quad n = 0, 1, \ldots, N-1 \tag{28}$$

where Ω_u denotes the uppermost frequency considered. The coefficients A_n are defined as

$$A_0 = 0 \quad , \tag{29}$$

$$A_1 = \sqrt{\left(\frac{1}{\pi}S(\Delta\Omega) + \frac{4}{6\pi}S(0)\right)\Delta\Omega} \quad , \tag{30}$$

$$A_2 = \sqrt{\left(\frac{1}{\pi}S(2\Delta\Omega) + \frac{1}{6\pi}S(0)\right)\Delta\Omega} \quad \text{and} \tag{31}$$

$$A_n = \sqrt{\frac{1}{\pi}S(\Omega_n)\Delta\Omega} \quad \text{for} \quad n = 3, 4, \ldots, N-1 \quad . \tag{32}$$

Applying this method of spectral representation the spectral power density functions yield efficiently the histories of the geometrical irregularities over the distance. Here the sample of a track is generated considering $N = 3540$ discrete frequencies up to $\Omega_u = 13.57\,\text{rad/m}$. The obtained data are used as input for the vehicle model discussed in this paper.

4 SIMULATION AND EVALUATION

The excitation by track irregularities affects the railway bogie. The resulting vibrations will be investigated by simulations and evaluated with respect to the stresses of the bogie frame. The scheme of the analysis is shown in Figure 5.

It is assumed that the railway vehicle is traveling with constant speed v. Then, the track irregularities are getting time dependent by the kinematic relation $x = vt$.

4.1 Simulation

The homogeneous linearized equations of motion (7) characterize the eigenbehaviour of the railway bogie. Table 1 shows the eigenfrequencies of the vertical submodel with corresponding eigenmodes while table 2 represents the results for the lateral submodel.

The eigenmodes can be divided into two groups. One group contains eigenmodes which describe the movement of the rigid bodies and the reference frame. The other group characterizes elastic degrees of freedom which describe the deformations. The eigenfrequencies of the second group differ from those observed on the free elastic bogie frame, see Figure 3, due to coupling phenomena.

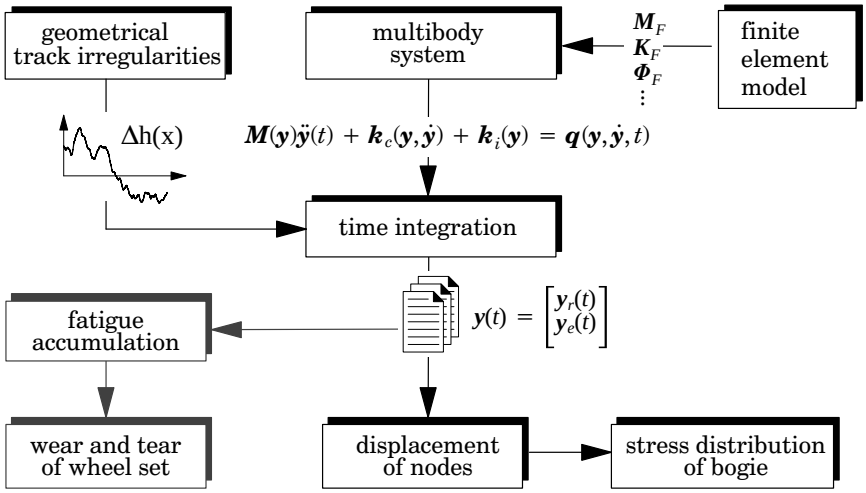

Figure 5: Scheme of the system analysis

The excitation is applied in the contact points of the wheels and rails. The vertical and lateral positions of these points are y_r, z_r, y_l, z_l. Here, the gauge deficiency is not considered and, hence, the lateral positions of the contact points of both wheels of one wheelset are identical. This implies $y_r = y_l = y_{r,l}$. The inversion of the equations (8), (9) and (10) gives the displacement of the left and right rail again as a function of the track characteristics

$$y_{r,l}(x) = \zeta_A(x) \quad , \tag{33}$$

$$z_r(x) = \zeta_V(x) - \zeta_C(x)/2 \quad \text{and} \tag{34}$$

$$z_l(x) = \zeta_V(x) + \zeta_C(x)/2 \quad . \tag{35}$$

As a result of the integration of the equations of motion the time histories of the generalized coordinates $\boldsymbol{y}$ are obtained, see also Figure 5. The time histories of generalized coordinates of both submodels are shown in Figure 6. There the displacements of the contact point (y_l, z_l) of the second wheelset, the coordinates of the car body (y_{CB}, z_{CB}) and the coordinates of the reference frame of the elastic car bogie (y_{BOG}, z_{BOG}) have the unit mm. Three vertical elastic coordinates ($z_{e,35}$, $z_{e,84}$, $z_{e,93}$) and two lateral elastic coordinates ($y_{e,101}$, $y_{e,110}$) are displayed multiplied by the factor 1000. The elastic deformations of the bogie seem to be small relative to the large motion in the degrees of freedom of the rigid car body and the reference frame of the bogie but they characterize the stresses.

The elastic coordinates describe the deformation of an elastic body and thus determine the displacement of the material points relative to the reference frame.

Table 1: Eigenfrequencies and eigenmodes of the vertical model

Eigenfrequency	**Eigenmode**
1.4 Hz	vertical mode of the car body
8.4 Hz	vertical mode of the bogie
9.9 Hz	roll mode of the bogie
11.8 Hz	pitch mode of the bogie
40.7 Hz 84.3 Hz 96.0 Hz 99.5 Hz 104.0 Hz	vertical modes of elastic deformation of the bogie frame

Table 2: Eigenfrequencies and eigenmodes of the lateral model

Eigenfrequency	**Eigenmode**
0.8 Hz	lateral mode of the car body
17.2 Hz	lateral mode of the bogie
59.5 Hz 101.0 Hz 110.0 Hz 112.0 Hz 125.0 Hz	lateral modes of elastic deformation of the bogie frame

However, these generalized elastic coordinates are difficult to discuss and to assess. Post-processing offers the possibility to describe interactions between the system components more precisely.

4.2 Evaluation

One of the goals of this paper is to show that the middle frequency motion may not be neglected for dynamic bending stress distributions. First the deflections of the nodes 1 and 2 of the bogie frame, see Figure 2, are discussed. On these nodes the external forces of the primary suspension are applied. The displacement history of node 1 and the corresponding power spectral density is shown in Figure 7 for the vertical motion. The displacement relative to the undeformed shape is expressed in coordinates of the bogie reference frame. The mean value of about -2.5 mm characterizes the static deformation due to gravitation. The maximum dynamic deviation from this mean value is about 0.7 mm which is about 25 % of the static deformation. The power spectral density shows two resonances in the range of low frequencies and two in the range of middle frequencies.

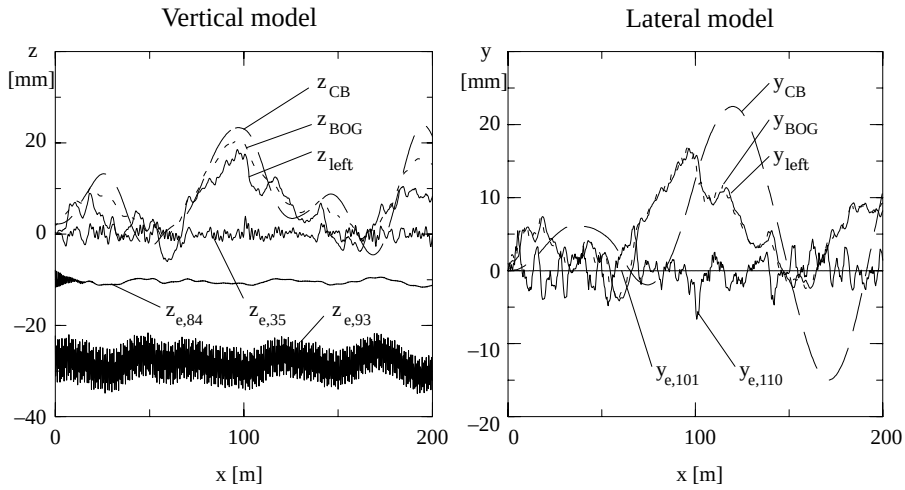

Figure 6: Time histories of generalized coordinates

The displacement of node 2 is shown in Figure 8 for the lateral motion. Here, the mean value is equal to zero since there is no static lateral force. The relatively small displacements are due to the high lateral stiffness of the bogie frame. The shape of the power spectral density shows resonances in the range of middle frequencies, too.

For the calculation of the dynamic stress distribution the time histories of the elastic coordinates are used. This method requires mode shape matrices which define the relation between these coordinates and the stress distribution. In this paper a static approximation is used to display the stress distribution due to the displacements of the nodes where the external forces of the suspension are applied. With the program ANSYS [3] static solutions are calculated for each time step. The obtained stress distributions are caused by the deflections of the nodes only and, hence, the effects due to the eigendynamics of the elastic bogie frame aren't included. Nevertheless, this approach indicates the stress distribution of critical parts of the bogie frame. Figure 9 shows the distribution of the v. Mises or equivalent stress at a specific time. The dark regions near to the head parts of the longitudinal griders indicate a high concentration of stress. Such a result was also obtained by Buse and Voß [2] who noticed high stress concentrations in these regions too.

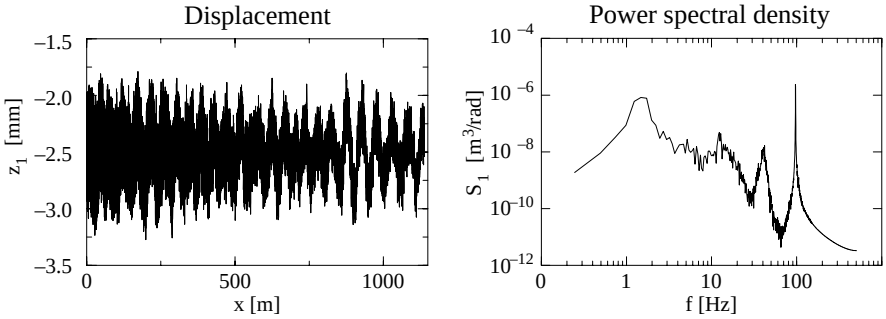

Figure 7: Displacement of node 1 in the vertical model

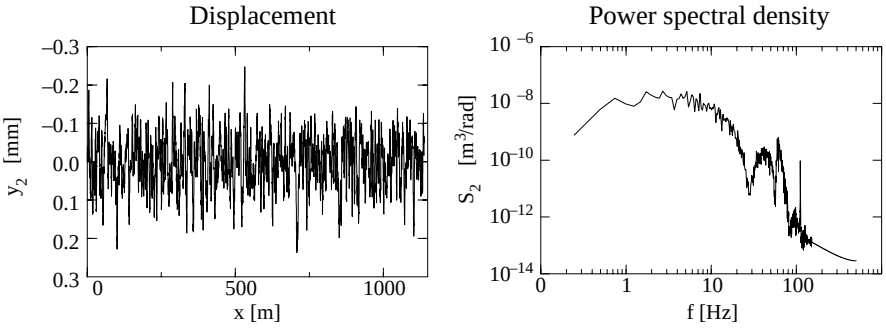

Figure 8: Displacement of node 2 in the lateral model

5 SUMMARY

The flexible multibody system approach assuming large gross motions and superimposed flexible deformations has been applied to the bogie MD 530 of the German ICE passenger coach. The eigenbehaviour of the railway bogie is analyzed and discussed. Power spectral density functions of measured geometric track irregularities are compared with analytical functions. Histories of track irregularities are obtained from analytical power spectral density functions applying a new method of spectral evaluation. These histories represent the properties of an average track and are available now for further investigation of the middle frequency dynamics.

Characteristic simulations of the railway bogie have been carried out and the results are discussed. Time histories and power spectral densities of the elastic deformations of the bogie frame from the undeformed shape are computed. They show elastic resonances in the range of low and middle frequencies. The quasi-static stress distribution in the bogie frame is calculated and regions of high concentration of stress are noticed.

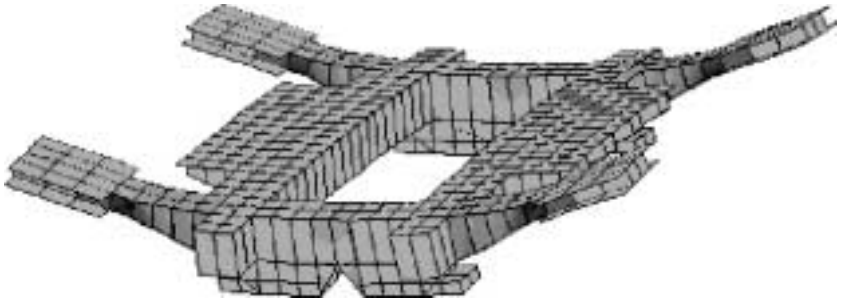

Figure 9: Stress distribution of the bogie frame for one time instant

The investigations reported in this paper show that the middle frequency motion may not be neglected in the analysis of dynamic bending and stress.

REFERENCES

1. Arbeitsgemeinschaft Rheine-Freren, "Rad/Schiene-Versuchs- und Demonstrationsfahrzeug, Definitionsphase R/S-VD", Ergebnisbericht der Arbeitsgruppe Lauftechnik, MAN, München, 1980.
2. Buse, H., Voß, G., "Lebensdauersimulation durch Betriebsfestigkeitsrechnung an Drehgestellen des Hochgeschwindigkeitsverkehrs", VDI-Berichte Nr. 1219, 1995, pp. 534–563.
3. DeSalvo, G. and Gorman, R., "ANSYS User's Manual", Swanson Analysis Systems, Houston, Pennsylvania, 1989.
4. Diepen, P., "Horizontaldynamik von Drehgestellen", Dissertation, TU Carolo-Wilhelmina, Braunschweig, 1991.
5. Ehrmann, F., "Methoden der Festigkeitsauslegung von Drehgestellrahmen im Wandel der Zeiten", In: ZEV+DET Glas. Ann. 115, Nr. 10, 1991, S. 303–315.
6. Guyan, R. J., "Reduction of Stiffness and Mass Matrices", AIAA Journal, Vol. 3, No. 2, 1965.
7. Hu, B. and Schiehlen, W., "On the simulation of stochastic processes by spectral representation", Prob. Engng. Mech. Vol. 12, No. 2, 1997, pp. 105–113.
8. Kreuzer, E. and Leister, G., "Programmsystem NEWEUL'90", Anleitung AN-25, Institute B of Mechanics, University of Stuttgart, 1991.
9. Luo, R. K., Gabbitas, B. L. and Brickle, B. V., "An Integrated Dynamic Simulation of Metro Vehicles in a Real Operating Environment", In: The Dynamics of Vehicles on Roads and on Tracks. Proc. 13th IVASD Symposium (Chengdu, 23–29 August 1993). Lisse: Swets & Zeitlinger, Vol. 23, 1993, pp. 334–345.
10. Melzer, F., "Symbolisch-numerische Modellierung elastischer Mehrkörpersysteme mit Anwendung auf rechnerische Lebensdauervorhersagen", VDI Fortschritt-Berichte, Reihe 20, Nr. 139, VDI-Verlag, Düsseldorf, 1994.
11. Popp, U. and Schiehlen, W., "Fahrzeugdynamik", Teubner-Verlag, Stuttgart, 1993.
12. Shabana, A. A., "Dynamics of Multibody Systems", Wiley, New York, 1989.
13. Shinozuka, M. and Deodatis, G, "Simulation of stochastic processes by spectral representation", Applied Mechanics Review, Vol. 44, 1991, pp. 191–204.

14. Stichel, S., "Betriebsfestigkeitsrechnungen bei Schienenfahrzeugen anhand von Simulationsrechnungen", VDI-Verlag, Düsseldorf, 1996.
15. Wallrapp, O., "Standard Input Data of Flexible Members in Multibody Systems", In: Schiehlen, W. (ed.): Advanced Multibody System Dynamics, Dortrecht: Kluwer Academic Publishers, 1993, pp. 445–450.
16. Wallrapp, O. and Eichberger, A., "FEMBS, An Interface between FEM Codes an MBS Codes, User Manual for ANSYS and NASTRAN", DLR, Oberpfaffenhofen, 1995.
17. Zacher, M., "Unrunde Räder und Oberbausteifigkeit", ETR 45, Nr. 10, 1996, S. 605–609.